Influence of Ca concentration on the electric, morphological, and structural properties of (Pb,Ca)TiO 3 thin films

F. M. Pontes, D. S. L. Pontes, E. R. Leite, E. Longo, E. M. S. Santos, S. Mergulhão, A. Chiquito, P. S. Pizani, F. Lanciotti Jr., T. M. Boschi, and J. A. Varela

Citation: Journal of Applied Physics **91**, 6650 (2002); doi: 10.1063/1.1470250
View online: http://dx.doi.org/10.1063/1.1470250
View Table of Contents: http://scitation.aip.org/content/aip/journal/jap/91/10?ver=pdfcov
Published by the AIP Publishing

Influence of Ca concentration on the electric, morphological, and structural properties of $(Pb,Ca)TiO_3$ thin films

F. M. Pontes, D. S. L. Pontes, E. R. Leite,[a] and E. Longo
LIEC–CMDMC, Department of Chemistry, UFSCar, Via Washington, Km 235, CP-676, CEP-13565-905, São Carlos, SP, Brazil

E. M. S. Santos, S. Mergulhão, A. Chiquito, P. S. Pizani, F. Lanciotti, Jr., and T. M. Boschi
Department of Physics, UFSCar, Via Washington, Km 235, CEP-13565-905, São Carlos, SP, Brazil

J. A. Varela
Institute of Chemistry, UNESP, Araraquara, SP, Brazil

(Received 28 November 2001; accepted for publication 25 February 2002)

$Pb_{1-x}Ca_xTiO_3$ ($0.10 \leqslant x \leqslant 0.40$) thin films on $Pt/Ti/SiO_2/Si(100)$ substrates were prepared by the soft solution process and their characteristics were investigated as a function of the calcium content (x). The structural modifications in the films were studied using x-ray diffraction and micro-Raman scattering techniques. Lattice parameters calculated from x-ray data indicate a decrease in lattice tetragonality with the increasing content of calcium in these films. Raman spectra exhibited characteristic features of pure $PbTiO_3$ thin films. Variations in the phonon mode wave numbers, especially those of lower wave numbers, of $Pb_{1-x}Ca_xTiO_3$ thin films as a function of the composition corroborate the decrease in tetragonality caused by the calcium doping. As the Ca content (x) increases from 0.10 to 0.40, the dielectric constant at room temperature abnormally increased at 1 kHz from 148 to 430. Also calcium substitution decreased the remanent polarization and coercive field from 28.0 to 5.3 $\mu C/cm^2$ and 124 to 58 kV/cm, respectively. These properties can be explained in terms of variations of phase transition (ferroelectric-paraelectric), resulting from the substitution the lead site of $PbTiO_3$for the nonvolatile calcium. © *2002 American Institute of Physics.* [DOI: 10.1063/1.1470250]

I. INTRODUCTION

Thin films of ferroelectric perovskites are of considerable interest both for fundamental research reasons and for their many actual and potential technological applications.[1,2] In recent years there is an increasing interest in lead titanate, $PbTiO_3$, with compositional modifications at Pb and Ti sites by Ca, Sr, La, and Zr, respectively, due to their potential applications, such as infrared sensors, electro-optic devices, ferroelectric memories and so on.[3–5] Among these materials, $(Pb,Ca)TiO_3$ (PCT) has recently attracted much attention for use in pyroelectric devices and ferroelectric memories, particularly as nonvolatile ferroelectric random access memories (NVFRAMs) due to the promise of high speed, radiation hardness, high remanent polarization, high dielectric constant, and low power consumption. Substitution of Pb for Ca, will introduce a shrinkage of the lattice in the c-axis direction of the tetragonal phase in the perovskite structure of $PbTiO_3$. Pure $PbTiO_3$ has a large tetragonal distortion at room temperature, $c/a \sim 1.064$, which will introduce a stress in the material upon the cooling through the phase transition, producing cracking in the material.[6] Therefore, the Ca substitution reduces the tetragonality (c/a), reducing the strain of pure $PbTiO_3$ thin films and inhibits cracking. Wang *et al.*[7] showed that sol-gel deposited PCT films exhibited a low tetragonal distortion and hindered the grain growth in the microstructure, both by means of the increase of the Ca content. Recent investigation of optical properties performed by Tang *et al.*[8] has shown that crystalline calcium-modified lead titanate thin films with different Ca contents (x) from 0 to 40%, prepared by the sol-gel process, presented a shift of the absorption edge toward a lower energy value, with the increase of Ca.

$Pb_{1-x}Ca_xTiO_3$ thin films have been prepared by a number of deposition techniques such as pulsed laser deposition,[9] sputtering,[10] sol-gel method.[11]

In this article, $Pb_{1-x}Ca_xTiO_3$ thin films with x from 0 to 0.40 are prepared by a soft solution processing, the so-called polymeric precursor method which can be used for the uniform deposition of polycomponent oxide films.[12–14] The effects of Ca content on the structural, electrical, and morphological properties of PCT thin films were systematically studied.

II. EXPERIMENT

In this study, the $Pb_{1-x}Ca_xTiO_3$ thin films with Ca contents corresponding to $x = 0.10$, 0.20, 0.30, and 0.40 were prepared by a soft solution method. The $(Pb,Ca)TiO_3$ precursor solution was synthesized using lead acetate trihydrate $[Pb(CH_3COO)_2 3H_2O]$, calcium carbonate ($CaCO_3$) and titanium (IV) isopropoxide $\{Ti(OCH(CH_3)_3)_4\}$ as starting materials. Titanium citrates were formed by the dissolution of

[a]Electronic mail: derl@power.ufscar.br

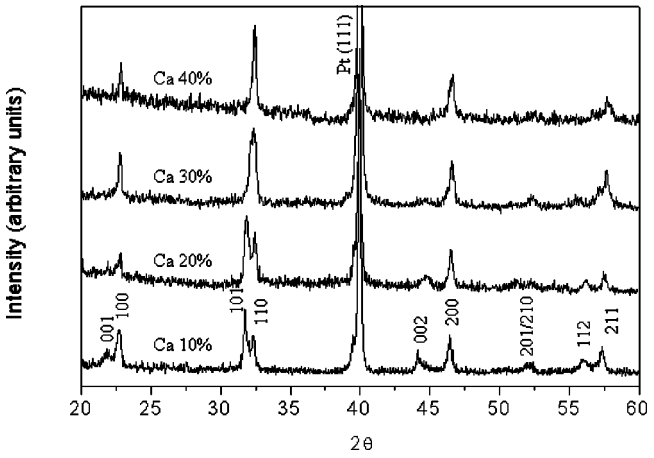

FIG. 1. X-ray diffraction patterns of $Pb_{1-x}Ca_xTiO_3$ thin films as a function of the Ca (x) content.

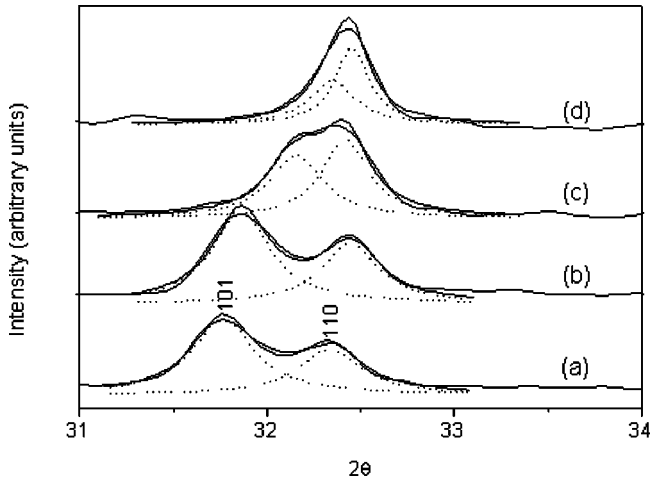

FIG. 2. Limited region x-ray data fitted to (100) and (001) reflections in $Pb_{1-x}Ca_xTiO_3$ thin films with different compositions: (a) $x=0.10$, (b) $x=0.20$, (c) $x=0.30$, and (d) $x=0.40$.

titanium (IV) isopropoxide in a water solution of citric acid (60–70 °C) under constant stirring to homogenize the Ti-citrate solution. Lead acetate trihydrate was dissolved in water, after which it was added, at a stoichiometric quantity, to the titanium citrate solution. Ammonium hydroxide was used to adjust the *p*H of the solution (*p*H 6–8) and to prevent precipitation of the lead citrate, which is favored in an acid solution. After homogenization, resulting in a clear solution, $CaCO_3$ was slowly added, while stirring vigorously. After homogenization of the solution containing Pb and Ca cations, ethylene glycol was added to promote mixed citrate polymerization by the polyesterification reaction. With continued heating at 80–90 °C, the solution became more viscous, albeit devoid of any visible phase separation. The viscosity of the deposition solution was adjusted to 15 mPa/s by controlling the water content. The polymeric precursor solution was spin-coated on substrates by a commercial spinner operating at 6000 rev/min for 20 s (spin-coater KW-4B, Chemat Technology). The polymeric precursor solution was deposited onto the substrates via a syringe filter to avoid particulate contamination. The substrate was Pt (140 nm)/Ti (10 nm)/SiO_2(1000 nm)/Si. After spinning onto the substrates, the films were kept in ambient air at 150 °C on a hot plate for 20 min to remove residual solvents. A two-stage heat treatment was carried out: initial heating at 400 °C for 2 h at a heating rate of 5 °C/min in an air atmosphere for the oxidation of residual organics, finally followed by heating at 600 °C for 2 h for the crystallization.

The film thickness was controlled by adjusting the number of coatings and each layer was oxidized at 400 °C and crystallized at 600 °C before the next layer was coated. These coating/drying operations were repeated until the desired thickness was obtained.

The (Pb,Ca)TiO_3 thin films were structurally characterized by x-ray diffraction (XRD) (Cu K_α radiation) in the mode of θ–2θ scan, recorded on a Siemens D5000 diffractometer. The lattice parameters of the (Pb,Ca)TiO_3 thin films were measured using the least-square method. The micro-Raman measurements were performed at room temperature in (Pb,Ca)TiO_3 thin films as a function of Ca content, using the 514.5 nm line of an argon ion laser as the excitation source. The power was kept at 15 mW and a 100× lens was used. The spectra were recorded using a T-64 Jobin-Yvon triply-monochromator coupled to a charge coupled device detector.

Atomic force microscopy (AFM) was used to obtain an accurate analysis of the sample surface and the quantification of very important parameters such as roughness and average grain size. A Digital Instruments Multimode Nanoscope IIIa (Santa Barbara, CA) was used. AFM imaging was carried out in the contact mode, using a triangular-shaped 200 μm long cantilever with a spring constant of 0.06 N/m. The scanning rate used ranged from 1 to 2 Hz and the applied force from 10 to 50 nN, depending on the sample/tip interactions. The film thickness was evaluated observing the cross-section of the films using a Zeiss DSM940A scanning electron microscopy.

The dielectric properties and capacitance–voltage curves were measured on films in a metal–ferroelectric–metal (MFM) configuration, using a HP4192A impedance/gain phase analyzer, and the hysteresis loop measurements were carried out on the films with a Radiant Technology RT6000HVS. These loops were traced using the "CHARGE 5" program included in the software of the RT6000HVS in a virtual ground mode test device. To measure electrical properties, Au dot electrodes of area 4.9×10^{-2} mm^2 were deposited by evaporation process on the surfaces of the fired films as top electrodes through a shadow mask, then a planar-type capacitor was fabricated. In order to achieve a contact with the platinum bottom electrode, a corner of the film was etched away using a HF+HCl solution. All the measurements were conducted at room temperature.

III. RESULTS AND DISCUSSIONS

According to x-ray diffraction analysis, the crystalline phase of the films was perovskite of tetragonal or pseudocubic structure, depending mainly on the Ca content, Fig. 1. For all thin films, a typical perovskite structure was observed with no second phase. In addition, this results is in agreement with the x-ray diffraction analyses for the powders of

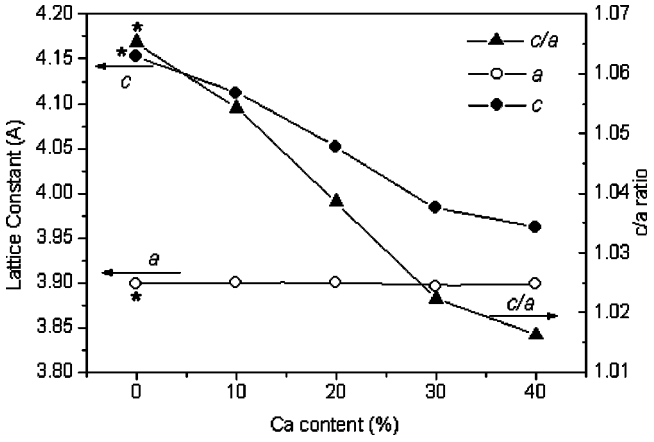

FIG. 3. Lattice parameter variations with Ca composition in $Pb_{1-x}Ca_xTiO_3$ thin films. Pure $PbTiO_3$ (reference).

the same composition and annealed at the same temperature. On the other hand, Tang *et al.*[8] observed that there are perovskite and pyrochlore phases coexisting in $Pb_{0.8}Ca_{0.2}TiO_3$ thin films, and there is only a pyrochlore phase in $Pb_{0.7}Ca_{0.3}TiO_3$ and $Pb_{0.6}Ca_{0.4}TiO_3$ thin films, all prepared the by sol-gel method and annealed at 650 °C. According to the (001)/(100) and (101)/(110) doublets, a tetragonal structure was formed by PCT(10) and PCT(20) thin films. However, a strong overlapping was observed for PCT(30) and PCT(40) thin films, showing a certain degree of tetragonality.

The possible effect of the overlapping of the PCT(30) and PCT(40) thin films has been attributed to the tetragonality decrease, (c/a), of the films with an increase of the Ca content, thus the structure was slowly transformed from tetragonal to pseudocubic. The limited 2θ (31°–34°) region in Fig. 2 clearly reveals the presence of (101) and (110) reflections in the x-ray patterns of these thin films. With increasing Ca content, the peaks slightly shifted towards higher angles. Figure 2 shows the deconvolution of the 101/110 peaks for PCT(10), PCT(20), PCT(30), and PCT(40) thin films, obtained by using the curve fitting program of the diffractometer. We can observe a gradual evolution with the increase of the Ca content, showing clearly that the PCT(30) films still possess the splits of the 101/110 peaks. On the other hand, PCT(40) films produce a broadening in the peak profile, indicating that possibly a pseudocubic structure is formed. Therefore, the peak splitting near $31° < 2\theta < 34°$, indicative of the tetragonal structure, tended to be merged and for $x > 0.40$, disappeared.

TABLE I. Frequency of the phonon modes in $Pb_{1-x}Ca_xTiO_3$ thin films as a function of Ca content at room temperature.

Mode	Frequency (cm^{-1})				
	$PbTiO_3$	$X=0.10$	$X=0.20$	$X=0.30$	$X=0.40$
$E(1TO)$	78	70	67		
$E(1LO)$	100			105	115
$A1(1TO)$	141				
$E(2TO)$	207	202	199	195	193
$B1+E$	288	286	284	277	273
$A1(2TO)$	330	325	316	292	277
$E(2LO)+A(2LO)$	449				
$E(3TO)$	504	516	523	532	546
$A1(3TO)$	608	596	590	572	572
$E(3LO)$	704				736

The variations in lattice parameters as a function of Ca content are shown in Fig. 3. The *a*-axis parameter showed only a slight decrease, remaining almost unchanged with increasing Ca content, while the *c*-axis parameter noticeably decreased. Figure 3 also shows the tetragonal distortion ratio, c/a, obtained from x-ray diffraction patterns for the PCT thin films, as a function of Ca content. The tetragonality decreased with the increasing of the Ca content.

The room temperature Raman spectra of PCT thin films with $x=0.10$, 0.20, 0.30, and 0.40 are compared with the pure $PbTiO_3$ thin film spectrum in Fig. 4. The main presence of the $E(1TO)$, $E(1LO)$, $A1(1TO)$, $E(2TO)$, $B1+E$, $A1(2TO)$, $E(2LO)$, $E(3TO)$, $A1(3TO)$, and $E(3LO)$

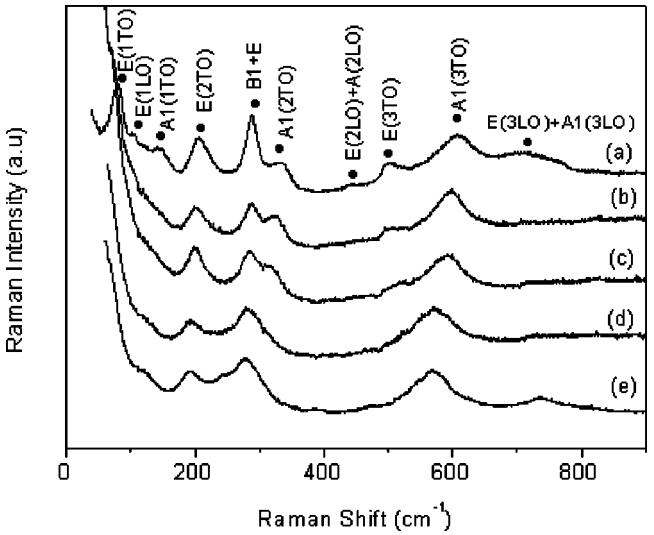

FIG. 4. Raman spectra of $Pb_{1-x}Ca_xTiO_3$ thin films at room temperature with different compositions: (a) undoped $PbTiO_3$ thin film reference, (b) $x=0.10$, (c) $x=0.20$, (d) $x=0.30$, and (e) $x=0.40$.

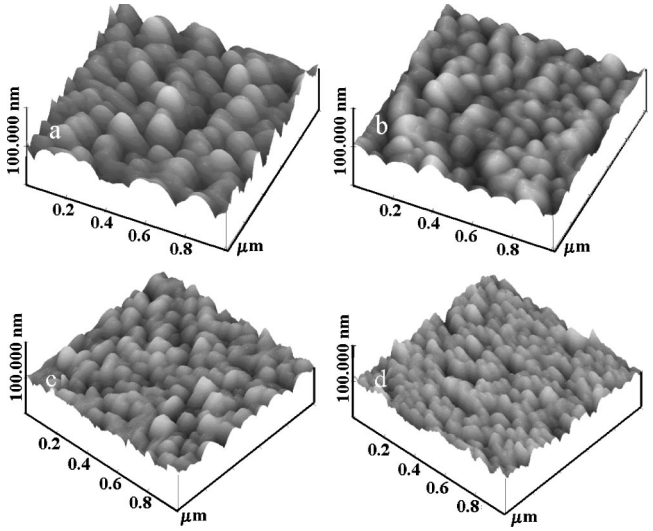

FIG. 5. Surface microstructure of the $Pb_{1-x}Ca_xTiO_3$ thin films heated at 600 °C for 2 h with different compositions obtained by atomic force microscopy: (a) $x=0.10$, (b) $x=0.20$, (c) $x=0.30$, and (d) $x=0.40$.

TABLE II. Evolution of parameters roughness and average grain size of the PCT thin films as a function of the Ca content.

	PCT(10)	PCT(20)	PCT(30)	PCT(40)
Roughness (nm)				
Average grain size (nm)	130	115	90	70

phonon modes in the Raman spectra indicates a tetragonal phase in these films. The softening of the $E(1TO)$ mode and the broadening of the Raman peaks increase with increasing Ca content in the $PbTiO_3$ lattice. This indicates that the incorporation of Ca content in the $PbTiO_3$ thin film lattice results in structural disorder in addition to the change in the crystalline structure. It is found that the $A1(2TO)-B1+E$ splittings of the Raman peaks and shift of the soft mode frequency agree with the tetragonality decrease for Ca content $x>0.20$. In addition, data from XRD analysis for Ca content, $x=0.40$, make that the crystal structure appears as pseudocubic, while Raman scattering revealed short-range tetragonal distortion order. The peak frequencies and the corresponding phonon modes for the PCT thin films compared with pure $PbTiO_3$ thin film are listed in Table I.

The evolution of the microstructure of PCT thin films, deposited on Pt-coated silicon substrates at a heating temperature of 600 °C, as a function of Ca content, is shown in Fig. 5. The average grain size was significantly reduced with the increase of the Ca content. In addition, overall observation of thin films indicate a good microstructure with no discontinuities in terms of pinhole and microcracks. Apparently, with the increase of Ca content, this morphology is still observed, becoming denser and smoother. The surface roughness and average grain size of PCT thin films measured by AFM are shown in Table II.

Electrical measurements were carried out for PCT(10), PCT(20), PCT(30), and PCT(40) thin films with 290, 260, 250, and 210 nm thicknesses, respectively.

Figure 6 shows the frequency dependence of the dielectric constant and tan δ at room temperature for the PCT thin films as a function of Ca (x) content. For the Ca richer samples, $x=0.30$ and $x=0.40$, the dielectric constant showed a slight tendency, to decrease with higher frequencies, although, for the samples of lower Ca content, $x=0.10$ and $x=0.20$, the dielectric constant showed to be insensitive to the frequency. The increasing tendency of tan δ was more pronounced at higher frequency ranges, over 10^6 Hz, several possible causes exist for such dispersion, including the hypothesis of the influence of the contact resistance between the probe and the electrode. Similar frequency dispersion behavior was also reported for other dielectric thin films.[15,16] The room temperature dielectric constant of the thin films greatly increased with increasing Ca contents as shown in Fig. 6. Such improvement in the dielectric properties of thin film is believed to be due to the transition from tetragonal to pseudocubic phase that takes place near room temperature as a result of the Ca substitution, which was confirmed by the results of the crystal structure analysis by XRD and Raman spectra, as shown in Figs. 1 and 4, respectively. In other words, the increase of the dielectric constant is related to the effect of the decrease of the Curie temperature (T_c) with increasing Ca concentration. Similar phenomena in the dielectric property have been reported for Sr and La substituted $PbTiO_3$ thin films.[4,17] Table III shows the dielectric constant of thin films studied measured at room temperature compared with other PCT thin films.

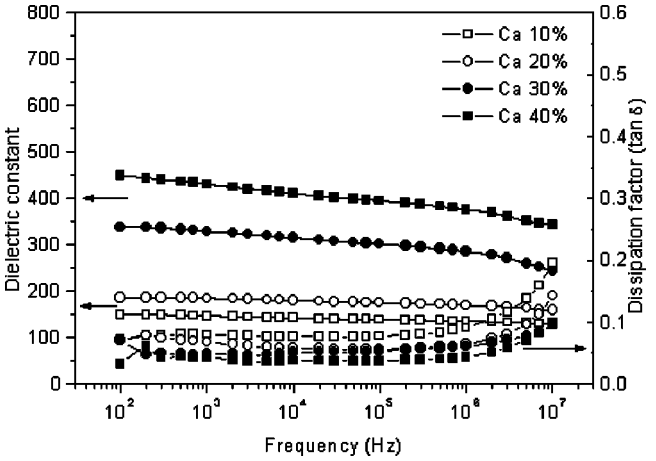

FIG. 6. Room temperature dielectric constant and tan δ of $Pb_{1-x}Ca_xTiO_3$ thin films with different Ca compositions as a function of the measuring frequency.

Figure 7 shows the capacitance–voltage characteristics ($C-V$) of PCT thin films deposited on $Pt/Ti/SiO_2/Si$ substrates, as a function of the Ca content and the dc bias applied voltage. The PCT thin film with Ca content of 0.10 showed two broad peaks, what characterizes a spontaneous polarization switching and the curve is symmetrically centered at about zero bias axis, a hysteresis behavior was ob-

TABLE III. Dielectric constant of PCT thin films herein obtained and according to the literature.

Process	PCT(10)	PCT(20)	PCT(30)	PCT(40)
Sputtering [a]	⋯	⋯	225 (100 kHz)	⋯
Sol-gel [b]	270 (1 kHz)	190 (1 kHz)	109 (1 kHz)	⋯
Sol-gel [c]	130 (1 kHz)	⋯	230 (1 kHz)	⋯
Sol-gel [d]	103 (1 kHz)	187 (1 kHz)	171 (1 kHz)	⋯
This study	148 (1 kHz)	184 (1 kHz)	329 (1 kHz)	430 (1 kHz)
	139 (100 kHz)	175 (100 kHz)	302 (100 kHz)	395 (100 kHz)

[a]See Ref. 18.
[b]See Ref. 19.
[c]See Ref. 20.
[d]See Ref. 21.

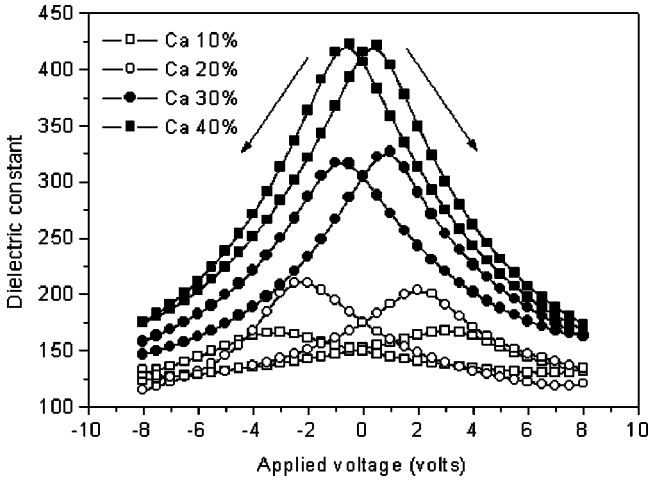

FIG. 7. The dependence of the dielectric constant of the PCT thin films on the Ca content and on the dc bias applied voltage.

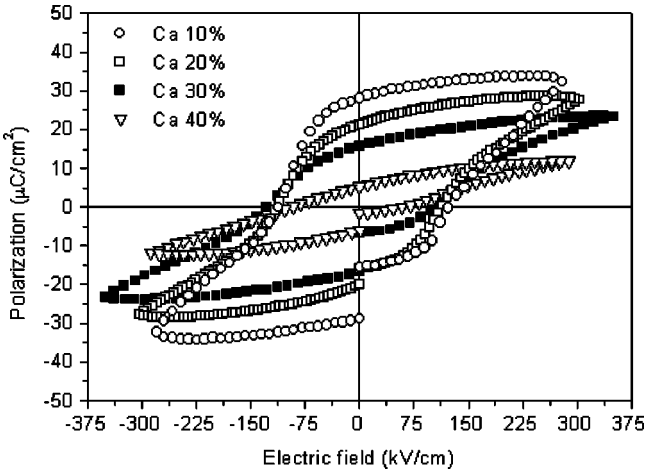

FIG. 8. $P-E$ hysteresis loops of $Pb_{1-x}Ca_xTiO_3$ thin films.

served. On the other hand, with the increase of Ca content (x) 0.20, 0.30, and 0.40, the separation between the curves of the positive sweep and negative sweep decreased, and the dielectric constant reached a maximum for the PCT(40) thin film. All curves are symmetrically centered at about the zero bias axis, what indicates that the films contain few movable ions or charge accumulation at the interface between the film and the electrode. In addition, the substitution of Ca in the lattice causes the reduction of the tetragonal distortion (c/a) and decreases the ferroelectric-paraelectric transition temperature (T_C).

The polarization versus voltage hysteresis loops were measured for the PCT thin films as a function of Ca content and are shown in Fig. 8. The polarization reached a maximum for the PCT(10) thin film and then the loops became slimmer with increasing Ca content. The coercive field decreased abruptly with the increase of the Ca content, indicating the increasing tendency of cubic or pseudocubic characteristics of the film structures. In addition, the observed decrease in polarization at higher Ca content is related to the fact that at these Ca substitution levels, the ferroelectric-paraelectric phase transition is being approached. Similar results for the Sr or La substituted $PbTiO_3$ thin films have shown that the composition for the maximum room temperature dielectric constant (or capacitance–voltage curves) nearly corresponded to those of ferroelectric-paraelectric phase transition. On the other hand, the maximum polarization was observed at the concentrations containing the lowest amounts of Sr or La.[17,22] Table IV summarizes our results of the remanent polarization and coercive field as a function of the Ca content, measured at room temperature compared with other PCT thin films.

IV. CONCLUSIONS

Polycrystalline $Pb_{1-x}Ca_xTiO_3$ thin films with different Ca contents, x varying from 0.10 to 0.40, have been deposited on $Pt/Ti/SiO_2/Si$ substrates, fabricated by a soft solution process. Raman spectra and x-ray diffraction analyses carried out $Pb_{1-x}Ca_xTiO_3$ thin films showed that the Ca addition results in a gradual decrease of tetragonality and considerable modification of Raman spectra and x-ray patterns. The broadening of the Raman peaks $[B1+E, A1(2TO)]$ remarkably increases with the increasing of Ca concentration in the $PbTiO_3$ lattice, indicating that the replacement of Pb by Ca induces structural disorder and changes abruptly the crystal structure. With increasing Ca concentration, the tetragonality of PCT thin films tended to decrease from 1.064 to 1.016. AFM analysis showed that the surface roughness and the grain size of PCT thin films decrease as the Ca concentration increases from x value of 0.10 to 0.40.

The electrical characteristics of the MFM capacitors with PCT thin films showed excellent dielectric and ferroelectric properties. Upon increasing the Ca concentration, the films became almost pseudocubic, resulting in the increase of

TABLE IV. Ferroelectric properties of PCT thin films herein obtained and according to the literature. P_r = remanent polarization ($\mu C/cm^2$); E_c = coercive field (kV/cm).

	PCT(10)		PCT(20)		PCT(30)		PCT(40)	
Process	P_r	E_c	P_r	E_c	P_r	E_c	P_r	E_c
Sputtering [a]					20.0	250		
Sol-gel [b]	13.5	125	13.0	110	7.5	80		
Sol-gel [c]	17.0	230	8.0	64	4.6	68		
This study	28.0	124	21.3	115	15.6	100	5.3	58

[a]See Ref. 18.
[b]See Ref. 19.
[c]See Ref. 21.

room temperature dielectric constant as well as in a slim type hysteresis loops. The dielectric constant at 100 kHz increased with the increasing Ca content of the films from 139 to 395. The $C-V$ characteristics of MFM capacitors showed hysteresis loop due to the ferroelectric switching property. On the other hand, the hysteretic behaviors decreased with increasing Ca content, what means a relatively easier switching of the domains with increasing Ca content, even with the decrease of the average grain size. The remanent polarization and coercive field decreased, due to the phase transformation from ferroelectric to paraelectric phase with the increasing Ca content, from $P_r = 28.01$ to 5.35 $\mu C/cm^2$ and $E_c = 123.00$ to 58.00 kV/cm, respectively.

These results showed a strong dependence of the morphological, structural and electrical properties of the PCT thin films on the Ca concentration. In addition, considering the presented results, Ca addition offers a good control over many of the desired room temperature dielectric and structural properties. Moreover, all the results show that $Pb_{1-x}Ca_xTiO_3$ ferroelectric thin films are promising materials for dynamic random access memories or NVFRAMs. It is believed that the dielectric, morphological, and structural qualities are resulted from the soft solution processing that uses aqueous solutions to create shaped, sized, and oriented materials, and also emphasizes low-energy routes to the synthesis of materials with desired chemical compositions and crystal structures.

ACKNOWLEDGMENTS

The authors gratefully acknowledge the financial support of the Brazilian financing agencies FAPESP, CNPq/PRONEX, and CAPES.

[1] A. D. Li *et al.*, J. Appl. Phys. **85**, 2146 (1999).
[2] Y. Watanabe, J. G. Bednorz, A. Bietsch, Ch. Gerber, D. Widmer, A. Beck, and S. J. Wind, Appl. Phys. Lett. **78**, 3738 (2001).
[3] J. Mendiola, M. L. Calzada, P. Ramos, M. J. Martin, and F. A. Rueda, Thin Solid Films **315**, 195 (1998).
[4] S. J. Kang, D. H. Chang, and Y. S. Yoon, Thin Solid Films **373**, 53 (2000).
[5] M. Es-Souni, M. Abed, A. Piorra, S. Malinowski, and V. Zaporojtchenko, Thin Solid Films **389**, 99 (2001).
[6] S. Y. Chu and C. Z. Chen, Sens. Actuators A **89**, 210 (2001).
[7] C. C. M. Wang, Y. T. Huang, Y. C. Chen, M. S. Lee, and M. C. Kao, Jpn. J. Appl. Phys., Part 1 **39**, 3579 (2000).
[8] H. Li, X. Tang, Q. Li, Y. Liu, Z. Tang, Z. Y. Zhang, and D. Mo, Solid State Commun. **114**, 347 (2000).
[9] M. J. Martín, J. Mendiola, and C. Zaldo, J. Am. Ceram. Soc. **81**, 2542 (1998).
[10] E. Yamaka, H. Watanabe, H. Kimura, H. Kanaya, and H. Ohkuma, J. Vac. Sci. Technol. A **6**, 2921 (1988).
[11] D. Bao, L. Zhang, and X. Yao, Appl. Phys. Lett. **76**, 1063 (2000).
[12] F. M. Pontes, E. Longo, E. R. Leite, and J. A. Varela, Thin Solid Films **386**, 91 (2001).
[13] F. M. Pontes, E. B. Araújo, E. R. Leite, J. A. Eiras, E. Longo, and J. A. Varela, Appl. Phys. Lett. **76**, 2433 (2000).
[14] V. Bouquet, M. I. B. Bernardi, S. M. Zanetti, E. R. Leite, E. Longo, J. A. Varela, M. Guilloux Viry, and A. Perrin, J. Mater. Res. **15**, 2446 (2000).
[15] P. C. Joshi and S. B. Krupanidhi, J. Appl. Phys. **72**, 5817 (1992).
[16] S. S. N. Bharadwaja and S. B. Krupanidhi, Thin Solid Films **391**, 126 (2001).
[17] D. H. Kang, J. H. Kim, J. H. Park, and K. H. Yoon, Mater. Res. Bull. **36**, 265 (2001).
[18] H. Maiwa and N. Ichinose, Jpn. J. Appl. Phys., Part 1 **36**, 5825 (1997).
[19] S. Chewasatn and S. J. Milne, J. Mater. Sci. **32**, 575 (1997).
[20] J. J. Shyu and K. L. Mo, J. Mater. Sci. Lett. **15**, 620 (1996).
[21] A. Tsuzuki, H. Murakami, K. Kani, K. Watari, and Y. Torri, J. Mater. Sci. Lett. **10**, 125 (1991).
[22] F. M. Pontes, J. H. G. Rangel, E. R. Leite, E. Longo, J. A. Varela, E. B. Araújo, and J. A. Eiras, J. Mater. Sci. **36**, 3565 (2001).